Bogdan SAPIŃSKI*

LINEARIZED CHARACTERIZATION OF A MAGNETORHEOLOGICAL FLUID DAMPER

SUMMARY

The paper is concerned with linearized characterization of a magnetorheological fluid (MR) damper. Two basic damping models, the equivalent viscous damping and the complex modulus, were used to linearize MR damper behaviour. The relationships between the parameters of the damping models were investigated experimentally in terms of the current applied to the damper coil and the maximal piston velocity.

Keywords*: MR damper, equivalent viscous damping, complex modulus*

LINEARYZACJA TŁUMIKA MAGNETOREOLOGICZNEGO

W artykule przedstawiono dwa modele tłumienia; równoważny współczynnik tłumienia wiskotycznego oraz moduł zespolony. Pierwszy z modeli reprezentuje tłumienie wiskotyczne, które jest związane z rozpraszaniem tej samej energii, jaka odpowiada faktycznemu mechanizmowi rozpraszania podlegającemu pomiarom. Drugi z modeli reprezentujący różne mechanizmy tłumienia ogólnie opiera się na racjonalizacji określenia tłumienia wiskotycznego wynikającego z teorii sprężystości. Oba modele wykorzystano do linearyzacji tłumika MR, którego cechują silnie nieliniowe charakterystyki, wynikające ze specyficznych właściwości cieczy MR wypełniającej tłumik. Modele te umożliwiają linearyzację tłumika MR, dzięki czemu może on być reprezentowany przez tłumik idealny w każdych warunkach pracy.

1. INTRODUCTION

The accurate modelling of damping leads to nonlinear terms and/or frequency, and temperature dependent ones that render the models difficult to use in vibration analysis. For this reason equivalent' linear viscous models have been developed which express the energy dissipated accurately, however, they do not capture the same physical behaviour.

In the study we focused on two damping models (equivalent viscous damping and complex modulus) that leads us to linearized models [2]. The equivalent viscous damping factor represents that level of viscous damping that dissipates the same energy as the actual mechanism which is being measured [1]. The complex modulus approach to various damping mechanisms is generally based on rationalization of viscous damping term that can be found in elasticity. These models are employed to linear characterization of MR damper whose inherent feature are high nonlinear characteristics being the result of special properties of MR fluid filling the damper [3]. This fact prompts many researchers to such MR damper model seek that makes its behavioural prediction possible. The explanation for these nonlinearities as well as MR damper models with various rheological structures has been widely discussed in the literature [8, 11]. The complexity of those models guarantees a reliable prediction of MR damper characteristics, however it makes the fast system evaluation quite a difficult task. For this reason, in the study, the MR damper is approximated by an ideal dashpot via introducing the coefficients of equivalent viscous damping and complex modulus. That allowed us to predict the damping and stiffness of the MR damper at every operating condition with a reasonable accuracy.

2. MR DAMPER

The force produced by a linear MR damper depends on magnetic field induced by the current in the damper coil and a piston velocity (Fig. 1). The damper operates in the flow mode and this means that the produced force is controlled by the flow resistance of MR fluid portion contained in the gap. As a magnetic field is applied to MR fluid in the damper, the damping characteristics of the fluid increase with practically infinite precision.

In the research program we used the MR damper of RD-1005-3 series manufactured by Lord Corporation (see Fig. 2). This damper is a small, compact shock absorber with simple electronics and low voltage, and currents demands that allow real-time damping adjustment [7].

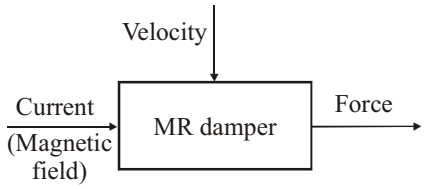

Fig. 1. Diagram for a MR damper

Fig. 2. RD-1005-3 damper

* Department of Process Control, AGH University of Science and Technology, Cracow, Poland, deep@agh.edu.pl

The damper has ±25 mm stroke. The input voltage is 12 V DC. The input current can be varied from 0 A to 2 A. The response time (dependent on amplifier and power supply) is less than 25 ms (time to reach 90% of maximal level during a 0 A to 1 A step input at velocity 51×10^{-3} m/s). The maximum extension force should be kept below 4448 N and operating temperature of the outer body should not exceed 71°C. The RD-1005-3 damper is particularly recommended for suspension in driver's seats in trucks, buses and farm tractors.

It was mentioned before that the inherent feature of MR damper are high nonlinear characteristics. This is illustrated in Figure 3, by experimental plots of force-displacement loops and force-velocity loops for RD-1005-3 damper measured at sine displacement excitation in the current range (0.0, 1.0) A [9]. Note that under this sine displacement excitation, the maximal piston velocity is 63×10^{-3} m/s.

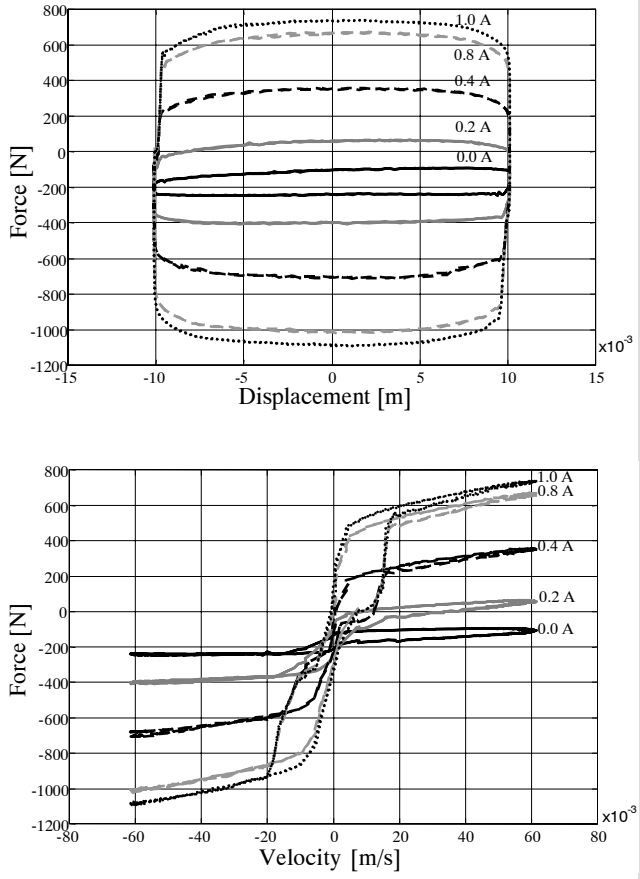

Fig. 3. Experimental data plots measured at sine excitation (frequency 1 Hz, amplitude 10×10^{-3} m), current: 0.0 A, 0.2 A, 0.4 A, 0.8 A, 1.0 A

It is readily apparent that:

- the force is not centered at zero (the effect of an accumulator containing high-pressure nitrogen gas),
- the greater current level, the greater force,
- the force increases much more for lower current levels (the effect of magnetic field saturation).

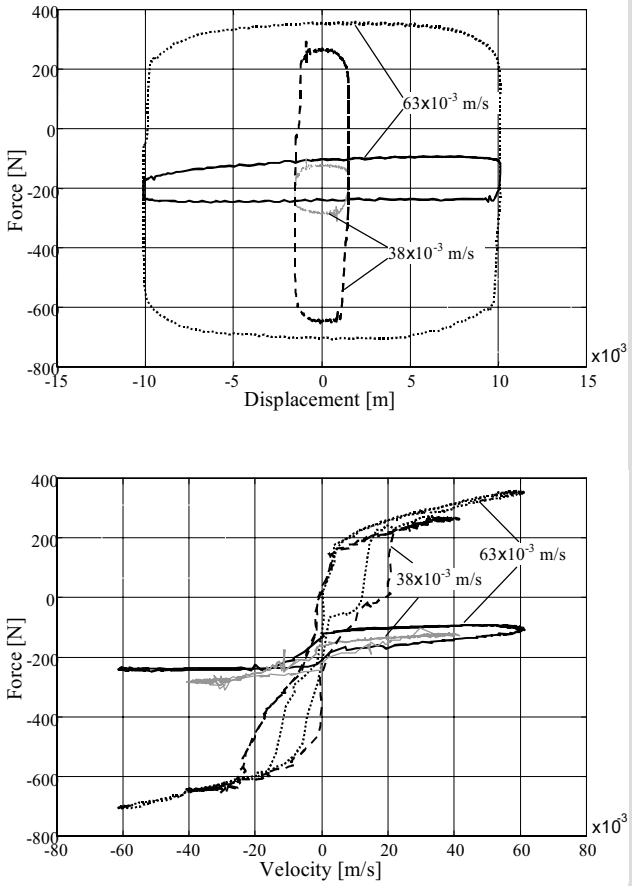

Fig. 4. Experimental data plots measured at sine excitations (frequency 1 Hz, amplitude 10×10^{-3}) and (frequency 4 Hz, amplitude 1.5×10^{-3} m), current: 0.0 A, 0.4 A

Let us compare the plots obtained under various sine excitation for two current levels 0.0 A and 0.4 A (see Fig. 4). Observing the plots we see that for each current, the peak to peak values of the force under sine excitation with frequency 4 Hz and amplitude 1.5×10^{-3} m (note that under this excitation, the maximal piston velocity is 38×10^{-3} m/s) are less than that under frequency 1 Hz and amplitude 10×10^{-3} m. It appears that at fixed current levels, the force varies due to maximal piston velocity which is a result of simultaneous change of frequency and amplitude of the applied excitation. This feature, equivalent to the capacity of the electro-hydraulic system of the vibrating testing machine restricts our considerations. For this very reason the introduced coefficient could not be investigated in terms of the excitation frequency and amplitude separately.

3. LINEARIZED CHARACTERIZATION – THEORETICAL BACKGROUNDS

To characterize MR damper we used the models of the equivalent viscous damping and the complex modulus which linearize the MR damper behaviour to be an ideal dashpot at every operating condition.

3.1. Equivalent viscous damping

When introducing the equivalent viscous damping we assume that the velocity of the MR damper piston $\dot{x}(t)$ is proportional to the restoring force $F(t)$, as given by the formula

$$F(t) = c_{eq}\dot{x}(t) \tag{1}$$

where c_{eq} is the equivalent viscous damping coefficient.

The coefficient c_{eq} is calculated using the energy dissipated by the MR damper over one cycle E. This energy can be found within the area enclosed by the force-displacement loop for the particular applied current and piston displacement. In the first approximation this area can be estimated, as the product of the peak to peak values of the piston displacement and the produced damping force, see the formula (2).That is because the obtained force-displacement plots are nearly rectangular in shape (see shaded area in Fig. 5).

$$E = 2\cdot(F_{\max} - F_{\min})\cdot X \tag{2}$$

Plots in Figure 3 reveal that a greater energy dissipated (a larger force-displacement loop) results from a higher level of applied current and the similar regularity is found for higher piston velocities.

Assuming sine displacement excitation $x(t) = X\sin\omega t$ (ω – driving frequency, X – amplitude), the energy dissipated by the MR damper over one cycle is given more precisely by the area enclosed within the hysteresis cycle given by following integral

$$E = \oint_l F dx = \int_0^{2\pi/\omega} F(t)\dot{x}(t)dt \tag{3}$$

The integral in the formula (3) corresponds to the grey area in Figure 5.

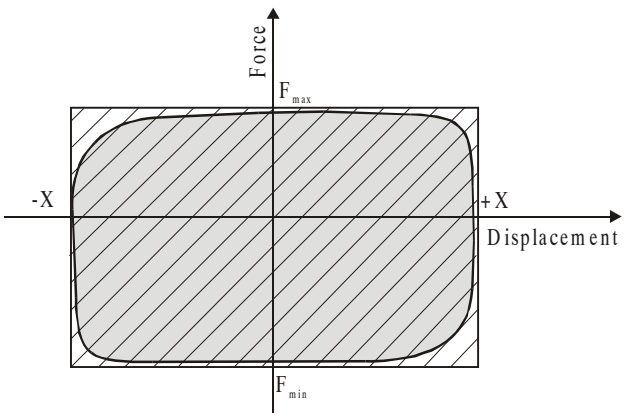

Fig. 5. Representation of energy dissipation by a MR damper over one cycle

An equivalent damping coefficient enables us to compare the damping performance of the MR damper with that of a viscous damper by equating the energy dissipated over one cycle

$$E = \int_0^{2\pi/\omega} c_{eq}\left[\dot{x}(t)\right]^2 dt = \int_0^{2\pi/\omega} c_{eq}(\omega X\cos\omega t)^2 dt = \\ = c_{eq}\pi\omega X^2 \tag{4}$$

and hence c_{eq} can be found as

$$c_{eq} = \frac{E}{\pi\omega X^2} = \frac{E}{\pi X(\omega X)} \tag{5}$$

The formula (5) implies that the equivalent viscous coefficient is a function of applied current and maximal piston velocity ωX, assuming that the excitation amplitude is fixed. Results achieved in experimental investigation of the relationship (5) are discussed in Subsection 4.2.

3.2. Complex modulus

When introducing the complex modulus we assume that both the force and displacement time histories are sinusoidal. The complex stiffness of the MR damper k^* has two components and can be written as

$$k^* = k_1 + jk_2 \tag{6}$$

The first component k_1, being an in-phase component (the real part of complex stiffness), is the storage stiffness. The second one k_2, being out of phase component (imaginary part of complex stiffness), is the loss stiffness. The components k_1 and k_2 can also be referred to as the effective stiffness and effective damping (damping modulus). The relationship between equivalent viscous coefficient c_{eq} and effective damping k_2 is not equivalent. That is because the effective damping involves only one harmonic frequency ω. The coefficients c_{eq} and k_2 are related by the following formula [4]

$$c_{eq} \approx \frac{k_2}{\omega} \tag{7}$$

The effective stiffness and effective damping can be calculated from the force produced by the damper $F(t)$ and the piston displacement $x(t)$. Assuming that

$$F(t) = F_s\sin(\omega t) + F_c\cos(\omega t) \tag{8}$$

and

$$x(t) = X_s\sin(\omega t) + X_c\cos(\omega t) \tag{9}$$

where F_s, F_c, X_s, X_c are Fourier coefficients of the force and the displacement $x(t)$ respectively.

The force-displacement relationship can be written as

$$F(t) = k_1 x(t) + \frac{k_2}{\omega}\dot{x}(t) \tag{10}$$

Substituting $F(t)$ and $x(t)$ in the formula (10) and equating the coefficients of sine and cosine terms, yields the effective stiffness and the effective damping:

$$k_1 = \frac{F_s X_s + F_c X_c}{X_s^2 + X_c^2} \tag{11}$$

$$k_2 = \frac{F_c X_s - F_s X_c}{X_s^2 + X_c^2} \tag{12}$$

The relationships (11) and (12) were investigated experimentally in terms of the applied current and the maximal piston velocity. The obtained results are discussed in Subsection 4.2.

4. LINEARIZED CHARACTERIZATION – EXPERIMENTAL INVESTIGATIONS

In order to investigate the relationships introduced in the previous section, the dynamic responses of the RD-1005-3 damper were measured under various sine displacement excitations in the current range (0.0, 1.0) A. The measurements were performed in the experimental setup described below.

4.1. Experimental setup

The schematic diagram of the experimental setup with the computer-controlled vibrating testing machine of Instron (model 8511.20) in which the RD-1005-3 damper was examined is depicted in Figure 6. The measurements were performed by the data acquisition system based on a PC with software provided by Instron. The RD-1005-3 damper ready for experiments is shown in Figure 7.

Piston displacement and force data at each assumed operating condition were acquired with a sampling frequency of 200 Hz for one cycle (a cycle is assumed as a full, up and down piston displacement), at the room temperature 22°C. Velocity data were computed by numerical differentiation. The capacity of the electro-hydraulic system of Instron machine was too small to change the excitation frequency at fixed amplitude and vice versa. Accordingly the relationships between equivalent viscous damping, effective stiffness and effective damping could be investigated only in terms of the applied current and the maximal piston velocity.

4.2. Results and discussion

Experimental data yield the relationships of equivalent viscous damping, effective stiffness and effective damping in terms of the applied current and the maximal piston velocity. Results of relevant computations are provided in Figures 8–13.

The relations in Figures 8 and 9 reveal that the coefficient c_{eq} increases with the increase of current (while the maximal velocity was kept fixed) and decreases with the increase of maximal velocity (while the current was kept fixed). In the first case the coefficient c_{eq} assumes its highest value when the maximal velocity is the lowest, the second case – when the applied current is the greatest. It seems that no matter what the value of velocity, there is a linear relationship between c_{eq} and the applied current in the range (0.0, 0.2) A.

Figures 10 and 11 show the coefficients of effective stiffness and effective viscous damping vs. current (the maximal piston velocity was kept fixed). The relations reveal that the coefficients k_1 and k_2 increase with the increase of current and they take larger values at higher values of maximal velocity. It seems that no matter what the value of velocity, there is a linear relationship between k_1 and k_2 and the applied current in the range (0.0, 0.2) A.

Figures 12 and 13 illustrate the coefficients of effective stiffness and effective viscous damping vs. maximal velocity (current was kept fixed). The relations reveal that the coefficients k_1 and k_2 decrease with the increase of velocity and they take larger value for higher levels of current. Note that at higher velocities the coefficients of effective stiffness and effective viscous damping depend on the current level in a minor degree only.

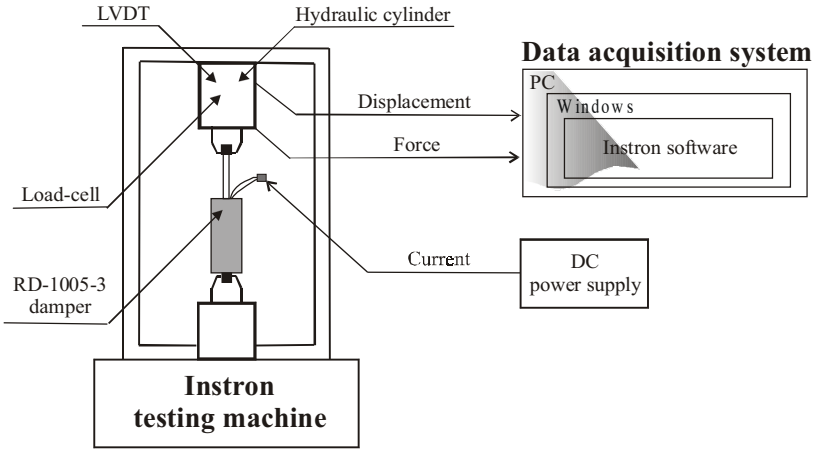

Fig. 6. Diagram of the experimental setup

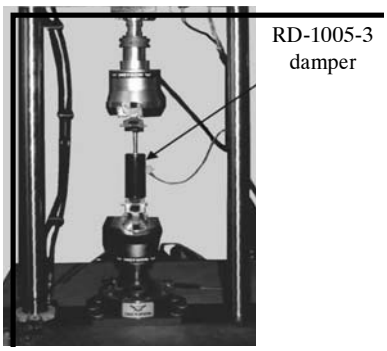

Fig. 7. RD-1005-3 damper in the Instron machine

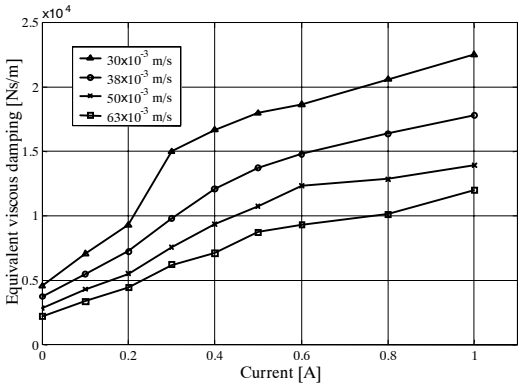

Fig. 8. Equivalent viscous damping vs. current

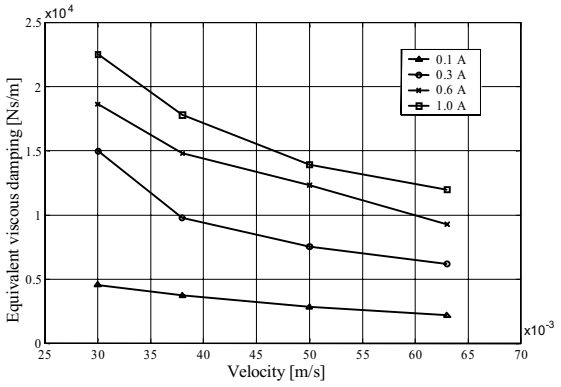

Fig. 9. Equivalent viscous damping vs. velocity

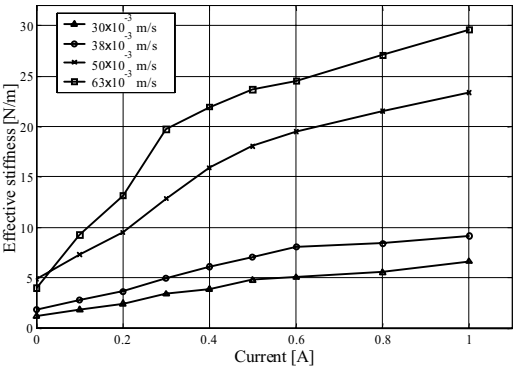

Fig. 10. Effective stiffness vs. current

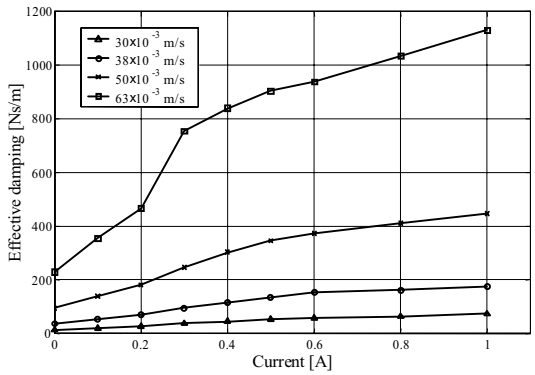

Fig. 11. Effective damping vs. current

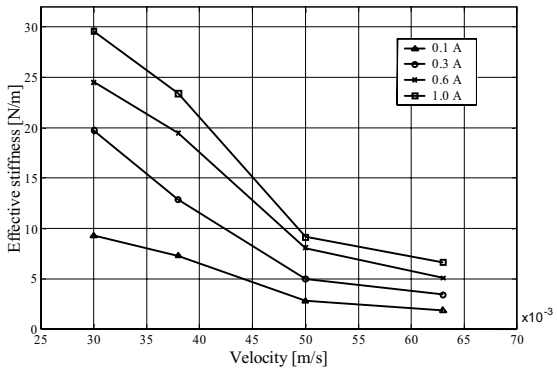

Fig. 12. Effective stiffness vs. velocity

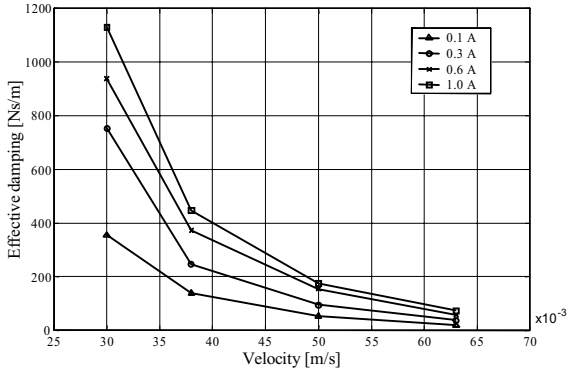

Fig. 13. Effective damping vs. velocity

5. CONCLUSIONS

Two basic damping models which linearize the MR damper behaviour were discussed in the study. The MR damper was approximated by an ideal dashpot at every operating condition. That allows us to predict its damping and stiffness with a reasonable accuracy. The introduced coefficients (equivalent viscous damping, effective stiffness, effective damping) were investigated experimentally in terms of the applied current and maximal piston velocity. Although the linearized characterization does not accurately portray hysteresis behaviour, these coefficients can be useful in validating a quasi-state model of a MR damper [10]. The determined values of equivalent viscous damping for RD-1005-3 damper are consistent with observations and comments having relevance to reports announced in [5] where the prototype model of RD-1005 damper was examined. Similar results were also provided in [6] where the model of RD-1005-1 damper was investigated. Note that results reported in [5] and [6] were obtained in terms of current, excitation frequency and amplitude.

Unfortunately the vibrating testing machine of Instron series available at the current research stage did not allow us to perform similar investigations and for this reason results reported in the study are presented strictly in terms of applied current and the maximal piston velocity.

Acknowledgement

The research is supported by the State Committee for Scientific Research as a part of the research program No. 4 T07B 016 26.

References

[1] Ewins D.J.: *Encyclopaedia of Vibration. Damping Measurement.* Academic Press, 2002, 332–335
[2] Inman D.: *Encyclopaedia of Vibration Damping Models.* Academic Press, 2002, 335–342
[3] Jolly M.R., Bender W., Carlson J.D.: *Properties and applications of commercial magnetorheological fluids.* Journal of Intelligent Material Systems and Structures, 10, 1999, 5–13
[4] Kamath G., Werely N.: *Dynamic characterization and analysis of magnetorheological damper behaviour.* Proc. of SPIE, 3327, 1999, 284–302
[5] Li W.H., Yao G.Z., Chen G., Yeo S.H., Yap F.F.: *Testing and Steady State Modeling of a Linear MR Damper under Sinusoidal Loading.* Journal of Smart Materials and Structures, 9, 2000, 95–102
[6] Liao W.H., Lai C.Y.: *Harmonic analysis of magnetorheological damper for a vibration control.* Journal of Smart Materials and Structures, 11, 2002, 288–296
[7] Lord Corporation. RD-1005-3 Product Bulletin, 2003
[8] Sapiński B., Filuś J.: *Analysis of Parametric Models of MR Linear Damper.* Journal of Theoretical and Applied Mechanics, 41, 2003, 703–722
[9] Sapiński B.: *Linear Magnetorheological Fluid Dampers for Vibration Mitigation: Modelling, Control and Experimental Testing.* Rozprawy Monografie, 128, Kraków, UWND AGH 2004
[10] Snyder R.A., Kamath G.H., Werely N.M.: *Characterization of a Magnetorheological Fluid Damper Using a Quasi-Steady Model.* Proc. of SPIE Con. on Smart Structures and Integrated Systems, 1999
[11] Spencer B., Dyke S., Sain M., Carlson J.: *Phenomenological model of a magnetorheological damper.* Journal of Engineering Mechanics, 1996